UCLA
UCLA Previously Published Works

Title

Plasticity of Myeloid Cells during Oral Barrier Wound Healing and the Development of Bisphosphonate-related Osteonecrosis of the Jaw*

Permalink

https://escholarship.org/uc/item/1tm9m71n

Journal

Journal of Biological Chemistry, 291(39)

ISSN

0021-9258

Authors

Sun, Yujie
Kaur, Kawaljit
Kanayama, Keiichi
et al.

Publication Date

2016-09-01

DOI

10.1074/jbc.m116.735795

Peer reviewed

eScholarship.org Powered by the California Digital Library
University of California

THE JOURNAL OF BIOLOGICAL CHEMISTRY VOL. 291, NO. 39, pp. 20602–20616, September 23, 2016
© 2016 by The American Society for Biochemistry and Molecular Biology, Inc. Published in the U.S.A.

Plasticity of Myeloid Cells during Oral Barrier Wound Healing and the Development of Bisphosphonate-related Osteonecrosis of the Jaw*

Received for publication, May 2, 2016, and in revised form, August 1, 2016 Published, JBC Papers in Press, August 11, 2016, DOI 10.1074/jbc.M116.735795

Yujie Sun[‡§¶1], **Kawaljit Kaur**[§‖], **Keiichi Kanayama**[§**], **Kenzo Morinaga**[§‡‡], **Sil Park**[§¶‖], **Akishige Hokugo**[§ §§], **Anna Kozlowska**[§‖¶¶2], **William H. McBride**[‖‖], **Jun Li**[‡3], **Anahid Jewett**[§‖4], **and Ichiro Nishimura**[§¶‖5]

From the [‡]*Department of Dental Implant Centre, Beijing Stomatological Hospital, School of Stomatology, Capital Medical University, Beijing 100050, China,* [§]*Weintraub Center for Reconstructive Biotechnology,* [¶]*Division of Advanced Prosthodontics, and* [‖]*Division of Oral Medicine and Biology, UCLA School of Dentistry, Los Angeles, California 90095,* [**]*Department of Periodontology, Asahi University School of Dentistry, Gifu, Japan 501-0296,* [‡‡]*Department of Oral Rehabilitation, Fukuoka Dental College, Fukuoka, Japan 814-0175,* [§§]*Division of Plastic and Reconstructive Surgery, David Geffen School of Medicine at UCLA, Los Angeles, California 90095,* [¶¶]*Department of Tumor Immunology, Chair of Medical Biotechnology, Poznan University of Medical Sciences, Poznan, Poland 61-866, and* [‖‖]*Division of Molecular and Cellular Oncology, David Geffen School of Medicine at UCLA, Los Angeles, California 90095*

Injury to the barrier tissue initiates a rapid distribution of myeloid immune cells from bone marrow, which guide sound wound healing. Bisphosphonates, a widely used anti-bone resorptive drug with minimal systemic side effects, have been linked to an abnormal wound healing in the oral barrier tissue leading to, in some cases, osteonecrosis of the jaw (ONJ). Here we report that the development of ONJ may involve abnormal phenotypic plasticity of Ly6G+/Gr1+ myeloid cells in the oral barrier tissue undergoing tooth extraction wound healing. A bolus intravenous zoledronate (ZOL) injection to female C57Bl/6 mice followed by maxillary first molar extraction resulted in the development of ONJ-like lesion during the second week of wound healing. The multiplex assay of dissociated oral barrier cells exhibited the secretion of cytokines and chemokines, which was significantly modulated in ZOL mice. Tooth extraction-induced distribution of Ly6G+/Gr1+ cells in the oral barrier tissue increased in ZOL mice at week 2. ONJ-like lesion in ZOL mice contained Ly6G+/Gr1+ cells with abnormal size and morphology as well as different flow cytometric staining intensity. When anti-Ly6G (Gr1) antibody was intraperitoneally injected for 5 days during the second week of tooth extraction, CD11b+GR1^{hi} cells in bone marrow and Ly6G+ cells in the oral barrier tissue were depleted, and the development of ONJ-like lesion was significantly attenuated. This study suggests that local modulation of myeloid cell plasticity in the oral barrier tissue may provide the basis for pathogenesis and thus therapeutic as well as preventive strategy of ONJ.

The major barrier tissues in mammals such as skin and intestinal mucosa segregate the host and external environments and withstand the frequent mechanical injury and microbial challenge with commensal as well as pathogenic species (1, 2). The highly active renewal capability of skin epidermis and intestinal epithelium affords rapid repopulation and recovery of barrier tissue continuity, and a repertoire of adaptive and innate immunity plays an essential role in the maintenance of barrier function and homeostatic relationship with microbes (3, 4). Barrier tissues maintain resident memory T cells (5, 6), innate lymphoid cells (7), and macrophages (8), which are highly specialized and capable of proliferating locally without contributions from distantly localized precursor cell populations. Infections and injuries to barrier tissues immediately activate the tissue-resident cells initiating the immune cascade.

Myeloid cells such as neutrophils are known to be the first respondent to the stressed barrier tissue, rapidly migrating into the affected tissue from the circulating peripheral blood population (9, 10). Unlike the resident immune cells in the barrier tissue, which express relatively predetermined functions, the infiltrating myeloid cells possess significant plasticity and are capable of undergoing substantial, rapid, and potentially reversible phenotypic and functional changes (11–14). The acquisition of plasticity plays an important role for the barrier immune system responding to various microenvironments influenced by microorganisms and frequent injury (15, 16). Abnormal plasticity of immune cells has been implicated as a cause of barrier tissue diseases (17, 18).

The lining mucosal membrane of the oral cavity presents a characteristic barrier tissue supporting the adaptive and innate barrier immunity. The oral environment is highly susceptible to commensal and pathogenic microbial challenge, mechanical irritation, and surgical wounding (19). Tooth extraction is one

* This work was supported, in whole or in part, by National Institutes of Health Grants R01 DE022552 and R21 DE023410 (NIDCR). This work was also supported, in part, by National Natural Science Foundation of China Grant 81371115. The authors declare that they have no conflicts of interest with the contents of this article. The content is solely the responsibility of the authors and does not necessarily represent the official views of the National Institutes of Health.

[1] Supported by the Joint Doctoral Training Program of Capital Medical University, Beijing, China.

[2] Recipient of "Mobility Plus" fellowship funded by Polish Ministry of Science and Higher Education.

[3] To whom correspondence may be addressed. E-mail: lijun3021@aliyun.com.

[4] To whom correspondence may be addressed. E-mail: ajewett@dentistry.ucla.edu.

[5] To whom correspondence may be addressed: Weintraub Center for Reconstructive Biotechnology, UCLA School of Dentistry, Box 951668, Los Angeles, CA 90095. Tel.: 310-794-7612; Fax: 310-825-6345; E-mail: inishimura@dentistry.ucla.edu.

of the most frequently prescribed surgical procedures, which leaves a large open wound of oral mucosa as well as a bony socket in the jawbone. Clinically, tooth extraction wounds heal with minimal scarring without complications, and the oral open wound is closed with the rapid approximation of oral mucosa (20, 21). The early immune respondent to the oral wound site is circulating neutrophils that are thought to play a pivotal role in regulating innate immunity, wound healing, and inflammation resolution (22, 23). However, oral barrier immunity and its functional role in responding to oral injury and infection are still largely unexplored.

Since the first report in 2003, osteonecrosis of the jaw (ONJ)[6] related to the medications preventing osteoclastic bone resorption has been recognized as extended chronic inflammation of oral barrier tissue and alveolar bone necrosis often associated with abnormal tooth extraction wound healing (24, 25). The intended target of anti-resorptive medications is the trabecular bone in the bone marrow environment of extremity and vertebral bones. Functional disturbance or differentiation of osteoclasts is achieved by bisphosphonates or humanized anti-RANKL antibody, respectively (26). Bisphosphonates primarily affect osteoclasts due to their strong affinity to bone minerals (27). After entering the system, bisphosphonates are rapidly adsorbed on the bone surface, whereas the rest in circulation is excreted within 24–48 h. Tooth extraction of bisphosphonate-treated patients has been shown to increase the prevalence of developing ONJ (28, 29). In bisphosphonate-treated rodent models, tooth extraction is associated with the development of osteonecrosis in the jawbone and prolonged chronic inflammation in oral barrier tissue (30, 31).

It has been indicated that bisphosphonates can be taken up by myeloid cells such as macrophages (32, 33), dendritic cells (34), and neutrophils (35, 36) and modulate their viability, migration, and function. This study addressed whether bisphosphonate-induced myeloid cell dysfunction might contribute to the pathological oral barrier immunity leading to the development of ONJ. Here we report that the aberrant Ly6G+/Gr1+ myeloid cell plasticity in the oral barrier tissue by intravenous injection of zoledronate (ZOL) is associated with the development of ONJ-like lesion at the tooth extraction site of mouse maxilla, whereas bone marrow myeloid cells remained unaffected. The ONJ-like lesion was significantly attenuated by Ly6G+/Gr1+ cell depletion through intraperitoneal injection of anti-Ly6G antibody. The outcome of this study suggests that the disturbance of myeloid cell plasticity significantly disrupts the oral barrier immunity and oral wound healing. This study further suggests that local modulation of myeloid cell plasticity in the oral barrier tissue may provide the basis for ONJ pathogenesis and thus a clue for the therapeutic and preventive strategy.

[6] The abbreviations used are: ONJ, osteonecrosis of the jaw; ZOL, zoledronate; KC, keratinocyte-derived chemokine; MIP-1α, -β, and -2, macrophage inflammatory proteins 1a, 1b, and 2, respectively; PMN, polymorphonuclear; HEMA, 2-hydroxylethyl methacrylate; CDDP, *cis*-diammine-dichloridoplatinum; micro-CT, micro-computed tomography; ROS, reactive oxygen species; TRAP, tartrate-resistant acid phosphatase; OC, osteoclasts; LIX, LPS-induced CXC chemokine.

Results

Development of ONJ-like Lesion in ZOL Mice—In mice, tooth extraction triggered a course of wound healing involving wound closure of the gingival oral barrier tissue and bone remodeling in the bony socket. Mice pretreated with a bolus IV injection of ZOL showed uneventful tooth extraction wound healing at day 3. However, the tooth extraction wound exhibited delayed healing at week 2, characterized by patent oral open wound (Fig. 1*B*) and delayed new bone formation in the extraction socket (Fig. 1*C*). Some ZOL mice exhibited abnormal bone formation at the external surface of alveolar bone near the tooth extraction site (*white arrow* in Fig. 1*C*), which appeared to persist in week 4. Histologically, a typical ONJ-like lesion in mice was composed of jawbone necrosis interfacing highly inflammatory gingival oral barrier tissue, occasionally developing pustule and fistula (Fig. 1*D*). Epithelial hyperplasia resulted in the abnormal epithelial cell contact to the necrotic bone surface or the exposure of jawbone to the oral cavity. The area of osteonecrosis in ZOL mice significantly increased at week 2 and persisted at week 4 (Fig. 1*E*). TRAP+ multinuclear osteoclasts were found on the surface of palatal bone as well as in the maxillary bone marrow (Fig. 1*F*). In some ZOL mice, osteoclasts appeared to be detached from the bone surface and "floating" in the oral barrier connective tissue. The number of osteoclasts was transiently increased at week 2 in both control (NaCl) and ZOL mice, whereas the number of osteoclasts was relatively consistent in the jawbone bone marrow space (Fig. 1*G*). These results were highly consistent with our previous report (31), and thus the ONJ mouse model was reproduced in this study. The effect of ZOL treatment resulting in the different tooth extraction wound healing appeared to be most significant at week 2.

The Effect of ZOL on Gingival Oral Barrier Immunity during Tooth Extraction Wound Healing—After tooth extraction, gingival oral barrier tissues were harvested and subjected to cell dissociation. The dissociated oral barrier cells were analyzed by flow cytometry. On day 3, week 2, and week 4, using gating strategy to account for all CD45+ cells, oral barrier tissues were found to contain ~60% CD45+ cells (Fig. 2*A*). However, the ZOL treatment increased the proportion of CD45+ cells (82%) during the active wound-healing period of week 2. It was also noted that the ZOL treatment developed a population with decreased CD45 staining intensity throughout the study period (Fig. 2*A*). Within CD45+ cells, CD3+ T cells consisted of ~8% to 10%, and the effect of ZOL on the T cell proportion was not observed (Fig. 2*B*). Our dissociation protocol appeared to be suitable to isolate oral barrier cells, giving rise to relatively consistent immune cell composition in the control (NaCl) and ZOL groups.

Dissociated oral barrier cells were cultured for 3 days, and the condition media were examined for the presence of cytokines and chemokines by a multiplex system (Fig. 2*C*). The secretion of granulocyte stimulating factor (G-CSF) and keratinocyte-derived chemokine (KC) was detected in day 3 oral barrier cells of control (NaCl) and ZOL mice, whereas macrophage inflammatory proteins 1α (MIP-1α) and 1β (MIP-1β), also known as CCL3 and CCL4, respectively, were

secreted more by ZOL cells. The gingival oral barrier cells of week 2 control (NaCl) mice exhibited a robust increase in the secretion level of cytokines and chemokines, such as G-CSF, Eotaxin (CCL11), granulocyte-macrophage colony-stimulating factor (GM-CSF), γ interferon (IFN-g), interleukins such as IL-6, IL-10, IL-12, and IL-13, LPS-induced CXC chemokine (LIX), and monocyte chemoattractant protein-1 (MCP-1). Strikingly, the oral barrier cells from week 2 ZOL mice had significantly impaired secretion of these cytokines and chemokines (Fig. 2*C*). The cytokine secretion diminished by the gingival oral barrier cells of week 4 control (NaCl) mice, whereas those cells from ZOL mice maintained high levels of G-CSF, KC, and macrophage inflammatory protein 2 (MIP-2) (Fig. 2*C*).

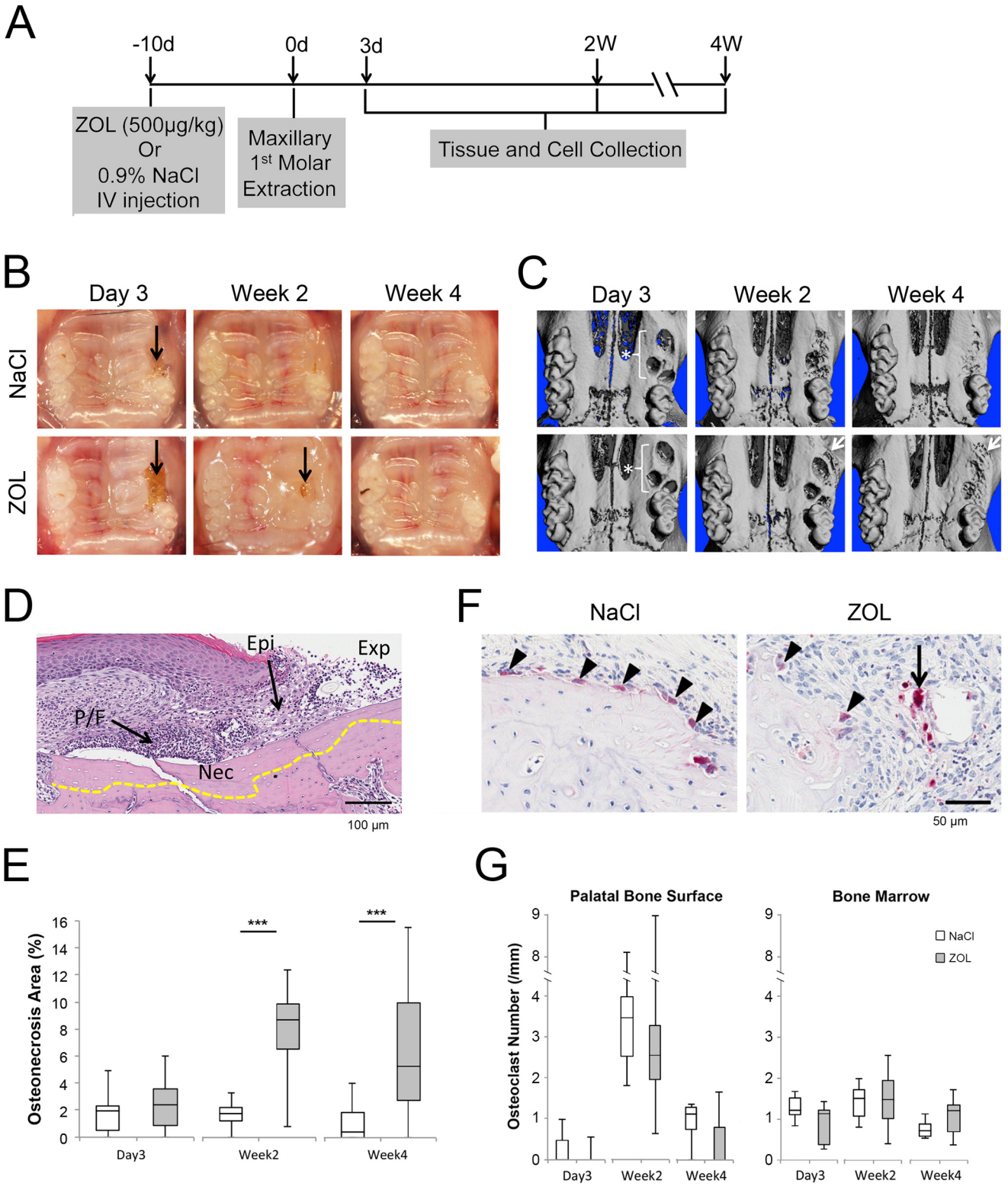

Ly6G/Gr1+ Myeloid Cells in Gingival Oral Barrier Tissue Were Modulated by ZOL Treatment—Immunohistochemical analysis revealed that polymorphonuclear (PMN) cells were positively stained with anti-Ly6G antibody in the gingival oral barrier tissue on day 3 and week 2 of tooth extraction of control (NaCl) mice (Fig. 3, *A* and *B*). Ly6G+ cells were clustered under the proliferating and migrating oral epithelium adjacent to the tooth extraction and separately at the deep connective tissue zone. ZOL mice on day 3 showed similar infiltration of Ly6G+ cells to the gingival oral barrier tissue as control, which picked up on week 2 (Fig. 3, *A* and *B*). It was observed that Ly6G+ cells were found in a close proximity to the alveolar bone, and osteoclasts in ZOL mice appeared to associate with immune cells including Ly6G+ cells (Fig. 3*A*). Ly6G+ cells in ZOL mice included small cells with condensed nuclear structure or large disintegrated cells (Fig. 3*D*).

The dissociated cells from gingival oral barrier tissues of week 2 control (NaCl) and ZOL mice were analyzed by flow cytometry. The back gating of control CD11b+Gr1^{hi} cells demonstrated a larger concentration of the CD11b+Gr1^{hi} population at the lower forward and side scatter area (gated area in the histogram) where the majority of myeloid population is expected to be seen; however, some cells can also be observed throughout the forward and side scatter histogram. When CD11b+Gr1^{hi} cell gate was applied to the dissociated cells of ZOL mice, the CD11b+Gr1^{hi} cells were apparently substantially decreased or missing (Fig. 3*C*).

The Condition Medium of Oral Barrier Cells from ZOL Mice-induced Necrosis of MLO-Y4 Cells in Vitro—A panel of cytokines/chemokines was shown to change expression in the dissociated oral barrier cells from ZOL mice. We tested if these modulated cytokines could influence osteonecrosis using murine osteocyte-like MLO-Y4 cells. In the initial study the majority of MLO-Y4 cells treated with 2-hydroxylethyl methacrylate (HEMA) acquired 7-aminoactinomycin D (*7AAD*) and annexin V-positive staining, suggesting their high sensitivity to HEMA-induced necrosis (Fig. 4*A*); however, MLO-Y4 cells were found relatively resistant to cisplatin (*cis*-diammine-dichloridoplatinum (CDDP))-induced apoptosis.

The overnight incubation with the condition medium of oral barrier cells dissociated from ZOL mice induced a fraction of necrotic propidium iodide (PI) +/annexin V+ MLO-Y4 cells that was almost twice as much of the control mouse oral barrier cell condition medium (Fig. 4*B*). Furthermore, MLO-Y4 cells with the ZOL mouse oral barrier cell condition medium demonstrated enlarged MLO-Y4 cells with pyknotic nucleus, which lost the typical dendritic processes (Fig. 4*C*). The altered morphology resembled osteocytes undergoing necrosis.

The Effect of ZOL and Tooth Extraction Wounding on Bone Marrow Myeloid Cells—It has been shown that myeloid cells in barrier tissues must be replenished from the circulating population, not from proliferating locally embedded cells. The primary therapeutic target of bisphosphonates is trabecular bone in the bone marrow of long bones and vertebral bones. Therefore, we postulated that the different response of Ly6G+/Gr1+ cells in the oral mucosa of ZOL-treated mice might be due to preconditioning in the bone marrow microenvironment. As expected, micro-computed tomography (micro-CT) evaluations showed increased trabecular bone volume (bone volume over tissue volume (*BV/TV*) and structural integrity (connectivity density (*Conn.D.*)) of mouse femurs after ZOL treatment (Fig. 5, *A* and *B*) (30, 31). Bone marrow flow through cells were harvested on day 3, week 2, and week 4 of tooth extraction and analyzed by flow cytometry. Anti-CD11b and anti-Ly6G antibodies generated various staining intensities. In the day 3 samples, CD11b^{int}Ly6G+ cells were predominant, whereas the week 2 samples contained mostly CD11b^{hi}Ly6G^{hi} cells (Fig. 5*C*). Overall, the ZOL treatment moderately decreased the bone marrow CD11b+Ly6G+ myeloid cells. When the same bone marrow cells were probed for Ly6C, the CD11b+Ly6C+ cells appeared to co-localize with CD11b+Ly6G+ cells in day 3 and week 2 samples (Fig. 5*D*). The ZOL treatment resulted in a moderate increase of CD11b+Ly6C+ cells in bone marrow. The intensity of the surface staining was substantially decreased in both CD11b+Ly6G+ and CD11b+Ly6C populations in week 4 compared with week 2 and day 3 in NaCl- and ZOL-treated mice (Fig. 5, *C* and *D*). Our data indicated that bone marrow myeloid cells appeared to be affected by oral wounding but not significantly influenced by ZOL.

Anti-Ly6G (Gr1) Antibody intraperitoneal (i.p.) Injection Eliminated Circulating CD11b+Gr1^{hi} Cells—ZOL mice appeared to develop ONJ-like lesions in the second week of tooth extraction, when Ly6G+ cells were abundant in the gingival oral barrier tissue. In this experiment, we addressed the role of oral barrier Ly6G+ cells on the development of ONJ. The control (NaCl) and ZOL mice were treated by daily i.p. injections of anti-Ly6G (Gr1) antibody in the second week from

FIGURE 1. **Abnormal tooth extraction wound healing in ZOL-treated mice.** *A*, time course schedule of mouse experiments. In all experiments, 7-week-old female C57BL/6 mice received a bolus IV injection of ZOL (500 μg/kg) or 0.9% NaCl vehicle solution. Ten days later, the maxillary left first molar was extracted. This protocol has been shown to generate ONJ-like lesion at the tooth extraction area of the maxilla of ZOL-treated mice (31). *B*, tooth extraction wound (*black arrow*) remained open on day 3 of the surgery in both vehicle-injected control (*NaCl*) and ZOL-injected (*ZOL*) mice. The oral barrier tissue wound was progressively closed in control mice; however, ZOL mice showed swelling and an open wound (*black arrow*) in the oral barrier tissue at week 2 of tooth extraction. The oral wound was healed by week 4 in both groups. *C*, reconstructed micro-CT images of day 3 samples showed the empty tooth extraction sockets (*), which were progressively filled with regenerating bone in control mice at week 2 and week 4. ZOL mice showed delayed bone regeneration in the extraction socket. In addition, some ZOL mice indicated the abnormal bone formation consistent with periosteal reaction (*white arrow*). *D*, a typical ONJ-like lesion in ZOL mice was composed of osteonecrosis (*Nec*) of alveolar bone interfacing the inflammatory oral barrier tissue or oral exposure site (*Exp*). Oral epithelium (*Epi*) contacted to the necrotic alveolar bone and formed pustule/fistula (*P/F*). *E*, the area of osteonecrosis composed of four or more empty osteocyte lacunae was equivalent at day 3 but increased in ZOL mice at week 2 and remained high at week 4 (day 3 NaCl, $n = 7$; day 3 ZOL, $n = 7$; week 2 NaCl, $n = 7$; week 2 ZOL, $n = 7$; week 4 NaCl, $n = 7$; week 4 ZOL, $n = 7$). ***, $p < 0.001$. *F*, TRAP+ osteoclasts appeared on the surface of alveolar bone interfacing the oral barrier tissue (*black arrowheads*) near the tooth extraction site. In ZOL mice, some TRAP+ osteoclasts (*black arrow*) were found detached from the bone surface. *G*, the standardized osteoclast number on the palatal bone surface increased at week 2 of tooth extraction in both control (NaCl) and ZOL mice, whereas the osteoclast number in the bone marrow space remained consistent. The osteoclast number was not different between control and ZOL mice except that in bone marrow at week 4. (day 3 NaCl, $n = 7$; day 3 ZOL, $n = 7$; week 2 NaCl, $n = 7$; week 2 ZOL, $n = 7$; week 4 NaCl, $n = 7$; week 4 ZOL, $n = 7$). ***, $p < 0.001$.

day 9 to day 13 of tooth extraction (Fig. 6*A*). The bone marrow flow through cells harvested on week 2 (the next day of the last anti-Ly6G (Gr1) antibody injection) generated the predominant CD11b+Gr1^{int} cell population at the expense of CD11b+Gr1^{hi} cells (Fig. 6*B*). This proportion was markedly contrasted with the antibody-untreated and the isotype

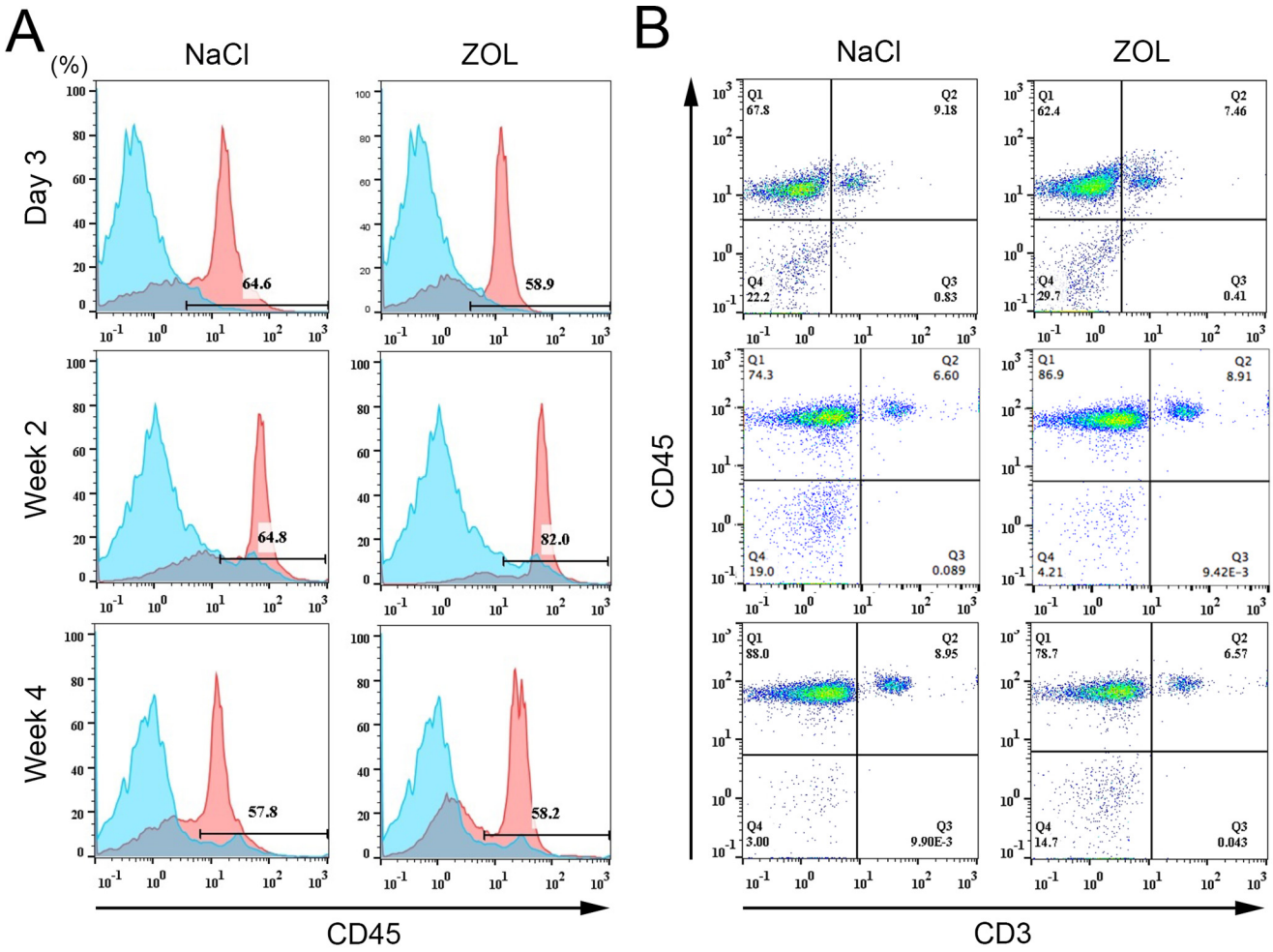

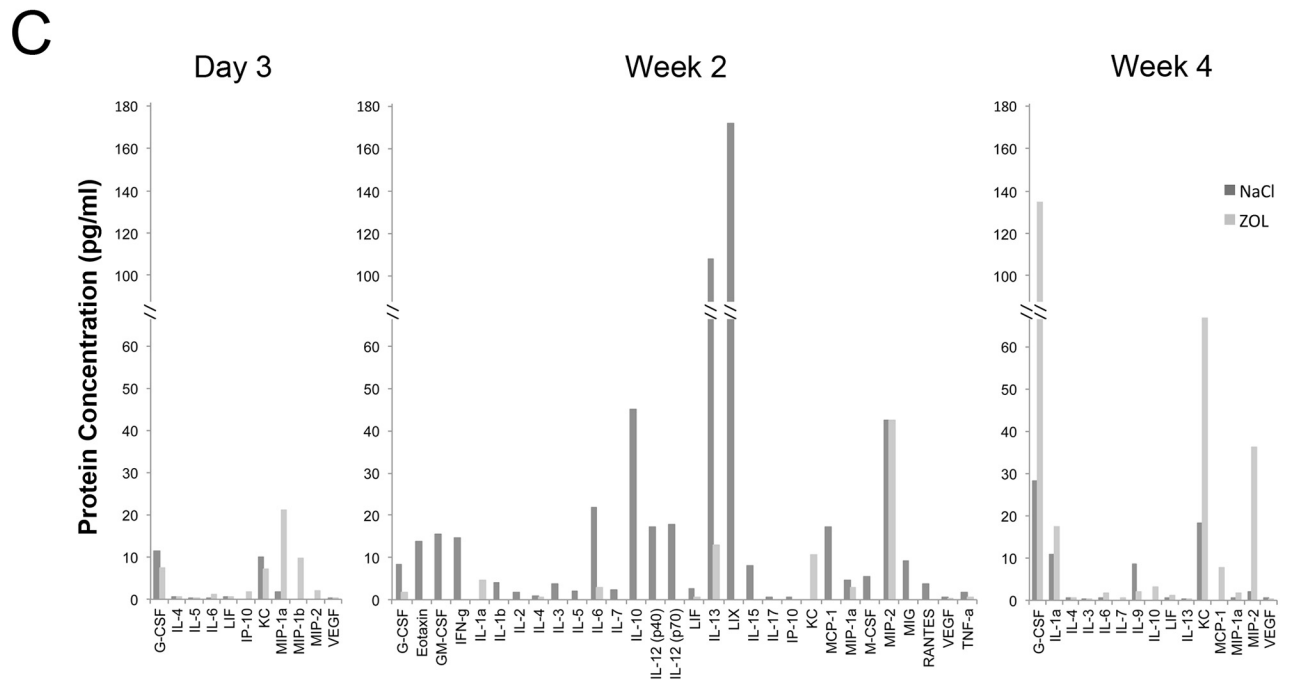

antibody-injected bone marrow samples, which showed CD11b+Gr1^{hi} cells or CD11b+Ly6G^{hi} cells as the predominant population, respectively (Fig. 6*B*). Peripheral blood samples harvested from the same animals showed that significant reduction of CD11b+Gr1^{hi} cells in the anti-Ly6G (Gr1) antibody-treated mice, whereas the antibody-untreated and the isotype antibody-injected groups identified the presence of CD11b+Gr1^{hi} cells or CD11b+Ly6G^{hi} cells, respectively (Fig. 6*C*).

Anti-Ly6G (Gr1) Antibody i.p. Injection during the Second Week of Tooth Extraction Wound Healing Prevented the Development of ONJ-like Lesion in ZOL Mice—When anti-Ly6G (Gr1) antibody was injected during the second week of tooth extraction, the tooth extraction wound healing was found nearly completed in not only control (NaCl) mice but more strikingly in ZOL mice (Fig. 7*A*). The swelling of gingival oral barrier tissue was observed in ZOL mice without the antibody treatment or with the isotype control antibody injection along with the open barrier tissue wound. These complications were not observed in all mice with the anti-Ly6G (Gr1) antibody injection (Fig. 7*A*). The histological osteonecrosis area of ZOL mice was larger than that of control (NaCl) mice; however, the anti-Ly6G (Gr1) antibody injection appeared to attenuate the development of osteonecrosis (Fig. 7, *B* and *C*).

Histological analysis revealed that the gingival barrier tissue of control (NaCl) and ZOL mice with the anti-Ly6G (Gr1) antibody injection showed little inflammatory cell infiltration (Fig. 7*C*). On the contrary, control (NaCl) mice with the isotype control antibody injection developed a localized inflammation at the tooth extraction socket and along the surface of the palatal bone. In addition to the localized inflammation, ZOL mice further developed a wide spread area of diffused inflammation, which interfaced with osteonecrosis lesion and epithelial hyperplasia (Fig. 7*C*). Immunohistochemical analysis indicated that Ly6G-positive cells were disproportionately localized in the abnormal diffused inflammation area of ZOL mice. In ZOL mice with the anti-Ly6G (Gr1) antibody injection, the gingival barrier tissue was free from Ly6G-positive cells (Fig. 7*D*). There were sporadic Ly6G-positive cells around the closing oral epithelial wound over the tooth extraction socket (data not shown).

Discussion

This study reports that the abnormal Ly6G+/Gr1+ myeloid cells were present in the oral barrier tissue of ZOL mice during the second week of tooth extraction, when ONJ-like lesion was developed. The striking observation was that the deletion of those Ly6G+/Gr1+ myeloid cells clearly attenuated if not prevented the development of ONJ in ZOL mice (Fig. 7). Here we propose that dysregulated myeloid cell plasticity in the oral barrier tissue may play an important role in the pathological process of ONJ.

Myeloid cells can undergo changes in the phenotype and function described as immune plasticity (37). Neutrophils are classically defined as PMN cells characterized by the high expression of Ly6G/Gr1 markers with the relatively low expression of Ly6C marker (38). However, flow cytometric analysis demonstrated the varying staining intensity of these markers providing the basis for differentiation and phenotypic plasticity. Myeloid cells expressing Gr1 marker at the intermediate intensity (Gr1^{int} cells) have been described as myeloid-derived suppressor cells (MDSC) (39, 40), which represent immature myeloid cells capable of suppressing T cell immunity (41). A recent report on subpopulations of circulating neutrophils described granulocytic myeloid-derived suppressor cells with the intermediate CD11b expression (Cd11b^{int}) (42). An evaluation of mouse splenic myeloid cells reported Ly6G^{hi} or Gr1^{hi} cells to be differentiated neutrophils (43).

In the present study bone marrow cells were suggested to undergo phenotypic change along the course of tooth extraction wound healing highlighting the CD11b^{int}Ly6G^{int} cell cluster on day 3 and the CD11b^{hi}Ly6G^{hi} (Fig. 5*C*) or CD11b ^{hi}Gr1^{hi} cell cluster (Fig. 6*B*) on week 2. The local injury and infection can regulate the development and differentiation of bone marrow myeloid cells through circulating cytokines and growth factors (44, 45). Therefore, it is highly conceivable that tooth extraction wounding could influence the phenotypic plasticity of bone marrow myeloid cells. It must be noted that the effect of ZOL treatment on the bone marrow myeloid cell differentiation appeared to be less significant than the tooth extraction wounding (Figs. 5 and 6).

During tooth extraction wound healing, Ly6G+/Gr1+ cells appeared in the gingival oral barrier tissue as early as day 3 as previously reported (46); however, the distribution of Ly6G+ cells in the gingival oral barrier tissue was different in ZOL mice (Fig. 3). Recruitment of myeloid cells to the peripheral tissue is influenced by cytokines and chemokines, such as eotaxin (47), LIX, KC, and MIP-2 (48). Separately, it has been reported that bisphosphonates impair neutrophil chemotactic activity (36, 49). Because the effect of ZOL on the myeloid cell population in bone marrow (Fig. 5*C*) and peripheral blood (data not shown) was not evident, the abnormal behavior of Ly6G+/Gr1+ cells might be specific to the oral barrier tissue.

We have previously demonstrated that osteoclast functions not only for bone resorption but also as a local immune regula-

FIGURE 2. **Oral barrier immunity during tooth extraction wound healing.** Palatal gingival tissues including wound area were harvested on day 3, week 2, and week 4 after tooth extraction, and cells were dissociated for flow cytometric analysis. Dissociated cells from two mice of each group were combined. The experiment was repeated at least three different sittings. The representative data were presented. *A*, CD45+ immune cells (*red*) were consistently composed of ~60% of the total population (*blue*, isotype control) of dissociated oral barrier cells in both control (NaCl) and ZOL mice. However, the ZOL treatment increased the proportion of CD45+ cells (82%) during the active wound-healing period of week 2. It was also noted that the ZOL treatment developed a population with decreased CD45 staining intensity throughout the study period. *B*, the proportion of T cells in CD45+ cells was found undistinguishable in control (NaCl) and ZOL mice. *C*, the dissociated cells were cultured, and the media collected after 3 days were evaluated by the multiplex cytokine/chemokine assay. In the control (NaCl) group, the number and the secretion levels of cytokines and chemokines were robustly increased by oral barrier cells dissociated on week 2 of tooth extraction. By contrast, cytokine and chemokine secretion by oral barrier cells of ZOL mice was much less on week 2, whereas some remained high on week 4. Those cytokines and chemokines with less than the detection limit were not presented. *RANTES*, regulated on activation normal T cell expressed and secreted; *LIF*, leukemia inhibitory factor; *MIG*, monokine induced by interferon-gamma.

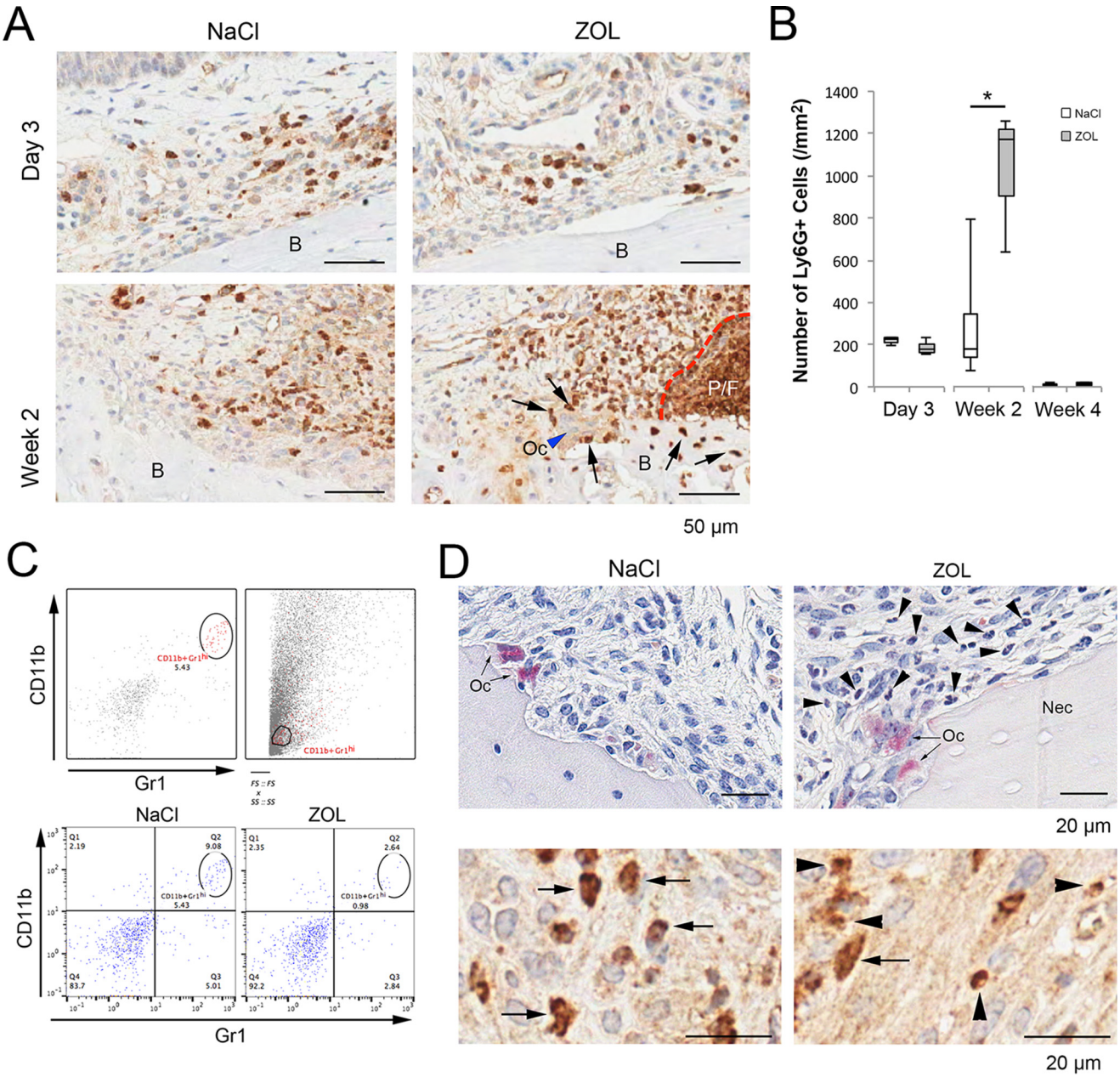

FIGURE 3. **Different Ly6G+ myeloid cells in the wound healing oral barrier tissue of ZOL mice.** *A*, immunohistology with anti-Ly6G antibody demonstrated clusters of Ly6G+ cells at the epithelial wound margin (not shown) and at the connective tissue interfacing palatal bone (*B*), both of which were adjacent to the tooth extraction site on day 3. In ZOL mice, fewer Ly6G+ cells were present in both cluster areas. At week 2, ZOL mice exhibited more Ly6G+ cells, in particular adjacent to jawbone oral exposure and/or pustule/fistula (*P/F*) areas. In some specimens, Ly6G+ cells (*arrows*) were found around osteoclast (*Oc*) and in necrotic bone (*B*). *B*, the number of Ly6G+ cells in the oral barrier tissue excluding the area of obvious jawbone exposure and P/F areas. *, $p < 0.05$; $n = 4$ in each group. *C*, flow cytometric analysis of the dissociated cells from oral barrier tissue harvested at week 2 of tooth extraction showed a large variation in size and granularity as shown in forward and side scatters. The back gating of CD11b+GR1^{high} cells revealed the significant reduction of these cells in ZOL mice. *D*, dense nucleus small cells (*arrowheads*) were characteristically associated with TRAP+ osteoclasts (*Oc*) and necrotic alveolar bone (*Nec*) in ZOL mice at week 2 of tooth extraction but not found in control (*NaCl*) mice. Ly6G+ cells in control (*NaCl*) mice were PMN cells (*arrows*), whereas Ly6G+ cells in ZOL mice included small cells that did not exhibit a typical PMN cell structure (*arrowheads*).

tor (50). The treatment with nitrogen-containing bisphosphonates, but not with non-nitrogen-containing bisphosphonate, significantly up-regulated the synthesis of proinflammatory cytokines by osteoclasts. Human γδ-T cells, when co-cultured with ZOL-pretreated osteoclasts, increased the synthesis of IFN-γ (31). The present study suggested that the apparent osteoclastogenesis on the palatal bone surface, the increased Ly6G+/Gr1+ cells in the oral barrier tissue, the significant down-regulation of cytokine and chemokine secretion, and the development of ONJ-like lesion occurred during week 2 in ZOL mice. These events may not be a mere coincidence. Although beyond the scope of this study, it is tempting to speculate that ZOL-affected osteoclasts may mediate the locally dysregulated plasticity of Ly6G+/Gr1+ myeloid cells in the oral barrier tissue, leading to abnormal oral barrier immune reactions and the development of ONJ. A mouse model of diabetes has shown a disproportionately high level of immature Gr1+myeloid cell population and abnormal phenotype development (51, 52). The

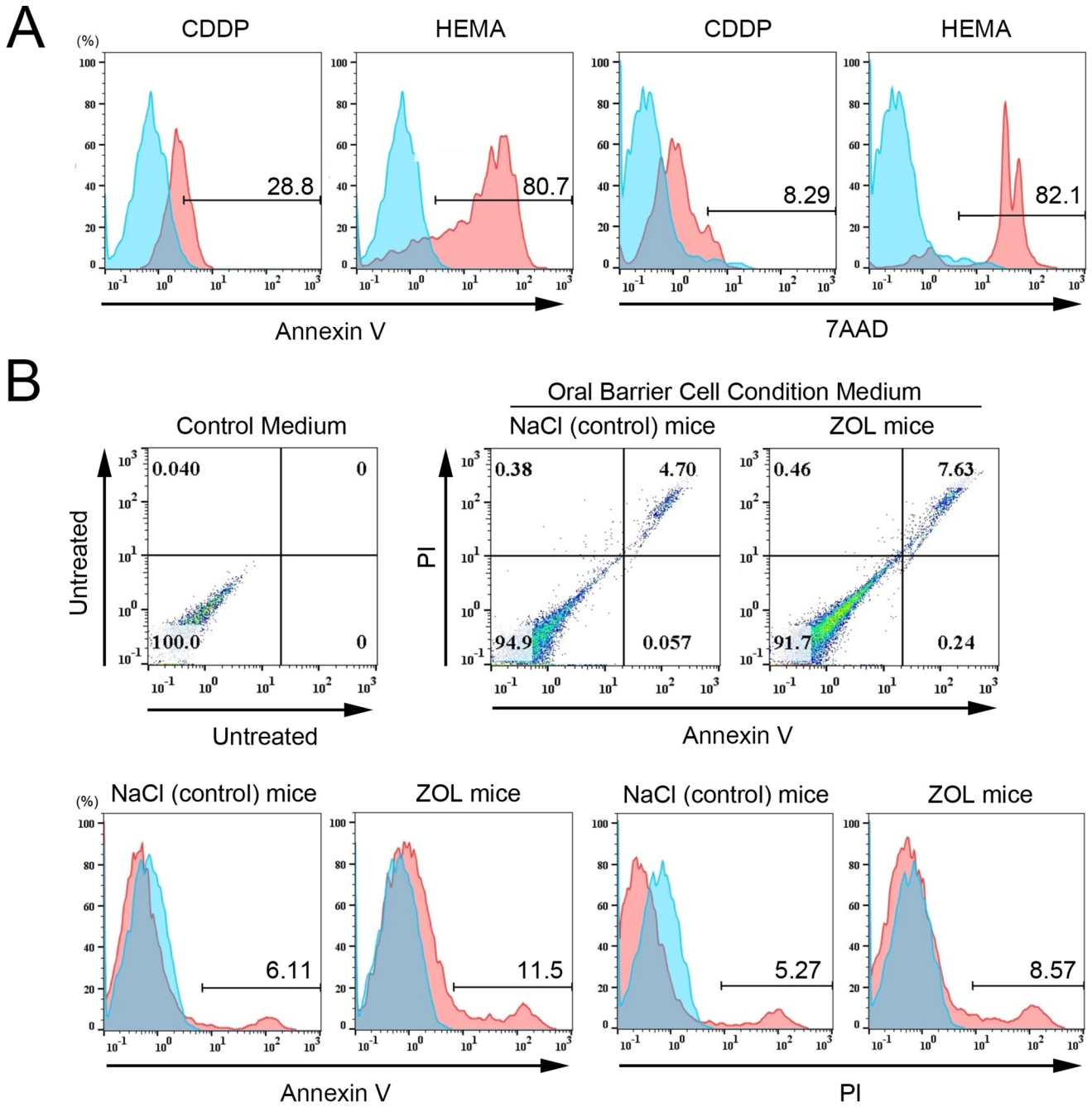
A
CDDP
HEMA
CDDP
HEMA
(%)
28.8
80.7
8.29
82.1
Annexin V
7AAD
B
Oral Barrier Cell Condition Medium
Control Medium
NaCl (control) mice
ZOL mice
Untreated
PI
0.040
0
100.0
0
0.38
4.70
94.9
0.057
0.46
7.63
91.7
0.24
Untreated
Annexin V
NaCl (control) mice
ZOL mice
NaCl (control) mice
ZOL mice
(%)
6.11
11.5
5.27
8.57
Annexin V
PI
C
Oral Barrier Cell Condition Medium
NaCl (control) mice
ZOL mice
HEMA

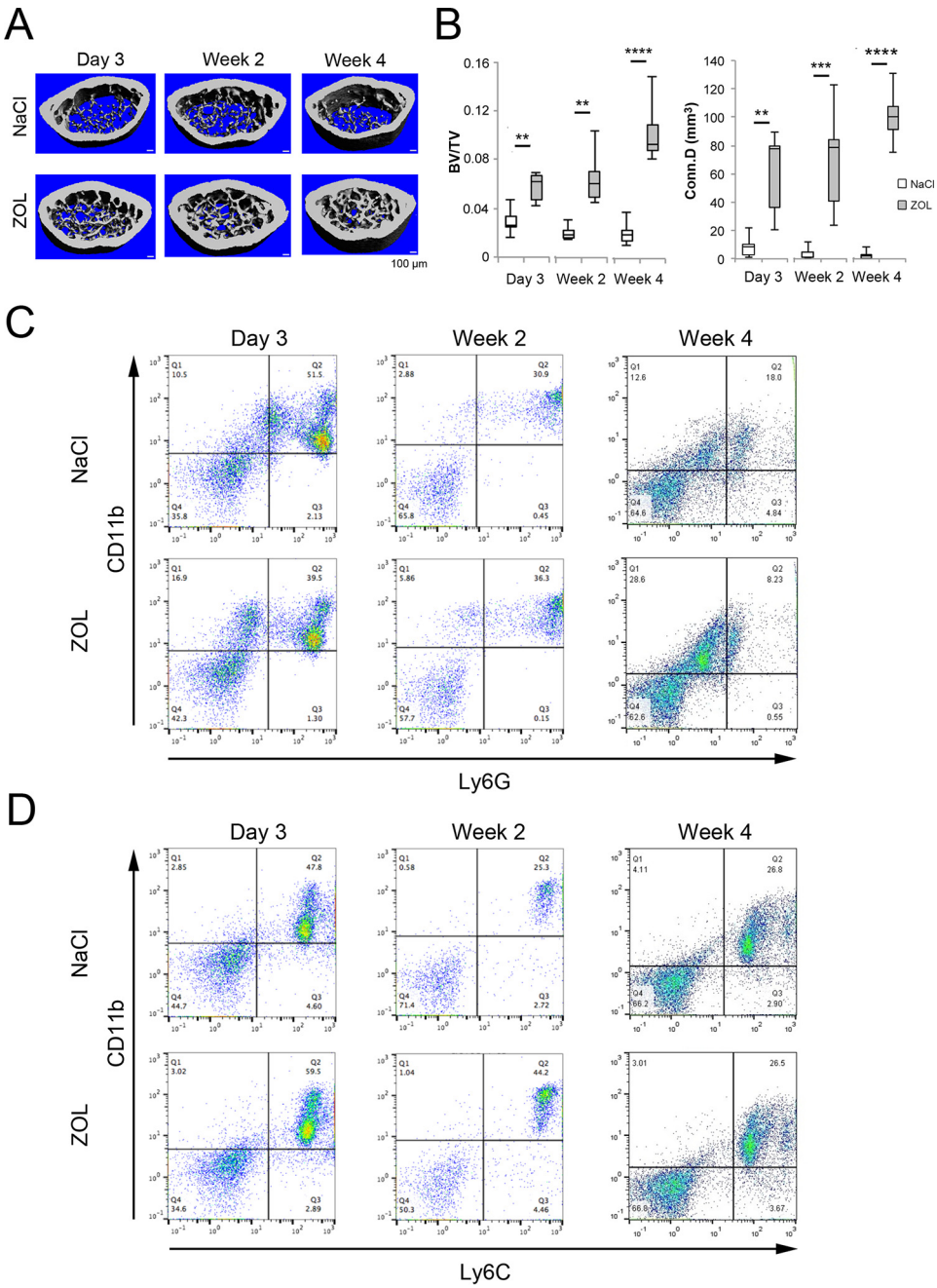

FIGURE 5. **Effect of ZOL on bone marrow myeloid cells.** *A*, 10 days after a bolus IV injection of 500 μg/kg ZOL, the maxillary first molar was extracted, and femur samples were harvested at day 3, week 2, and week 4 of tooth extraction. Reconstructed micro-CT images of the distal epiphyseal trabecular bone indicated the increased bone structure in ZOL mice. *B*, micro-CT quantitative measurements indicated the significant and progressive increase of femur trabecular bone structure in ZOL mice as depicted by bone volume/tissue volume (*BV/TV*) and connectivity density (*Conn.D*). **, $p < 0.01$; ***, $p < 0.001$; ****, $p < 0.0001$; $n = 7$ in each group. *C*, the total cell gate flow cytometric analysis of bone marrow flow through cells identified CD11b+ and Ly6G+ cells with various staining intensity during the tooth extraction wound healing period. At week 4, a noticeable decrease of CD11b+Ly6G+ cells in the ZOL group was indicated as compared with the control (*NaCl*) group. *D*, the bone marrow cells were proved for CD11b+ and Ly6C+ cells. The variation in staining intensity was observed. In day 3 and week 2, CD11b+Ly6C+ cells appeared to moderately increase in the ZOL group.

increased susceptibility of bisphosphonate-treated diabetes patients to develop ONJ (24, 25) may be explained, in part, by the underlining inability in myeloid cell plasticity.

We further demonstrated that the number of Ly6G+ cells in the gingival oral barrier tissue of ZOL mice was significantly increased at week 2 (Fig. 3*B*) and that the size and shape of

FIGURE 4. **Murine osteocyte-like MLO-Y4 cell necrosis *in vitro*, induced by condition medium of oral barrier cells dissociated from ZOL mice.** *A*, MLO-Y4 cells demonstrated the high sensitivity to HEMA-induced necrosis assessed by annexin V/7-aminoactinomycin D (*7AAD*)-positive staining. By contrast, MLO-Y4 cells were relatively resistant to CDDP-induced apoptosis. *B*, MLO-Y4 cells exposed to the condition medium of ZOL mouse oral barrier cells showed the increased necrotic reaction more than those exposed to the condition medium of control (*NaCl*) mouse oral barrier cells. *PI*, propidium iodide. *C*, MLO-Y4 cells exposed to the control (*NaCl*) mice oral barrier cell condition medium maintained the typical fibroblastic morphology with dendritic processes. The overnight incubation with the ZOL mice oral barrier cell condition medium induced enlarged cell morphology with pyknotic nucleus, which lacked dendritic processes (*white arrows*). The exposure to HEMA resulted in necrosis of the majority of MLO-Y4 cells.

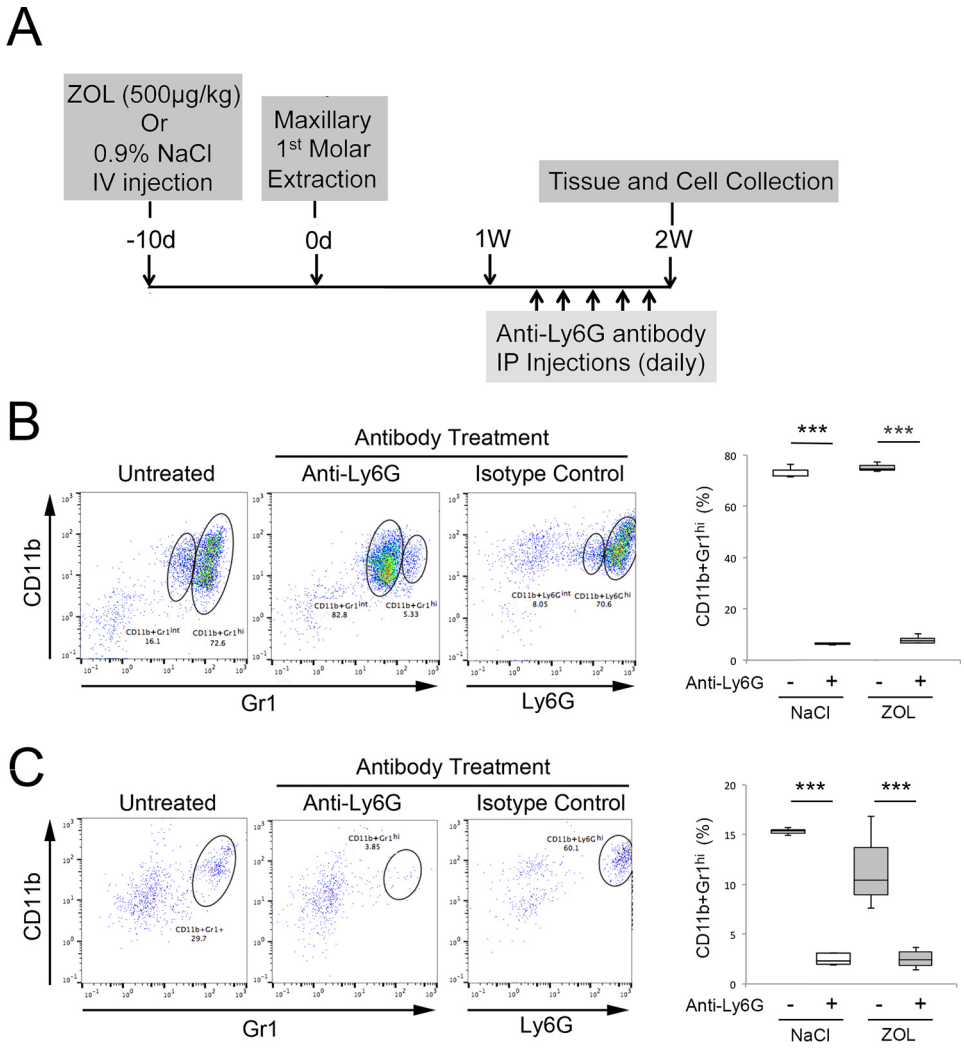

FIGURE 6. **Effect of anti-Ly6G (Gr1) neutralizing antibody injection on bone marrow and peripheral blood.** *A*, after a bolus IV injection of ZOL (500 μg/kg) or 0.9% NaCl vehicle solution and maxillary molar extraction, daily i.p. injections of anti-Ly6G (Gr1) neutralizing antibody (300 μg/animal/day) were performed starting from day 9 to day 13 of tooth extraction. Bone marrow flow-through cells and peripheral blood samples were harvested 1 day after the last anti-Ly6G (Gr1) antibody injection or on week 2 of tooth extraction. *B*, flow cytometric analysis of myeloid cell gate of bone marrow flow-through cells indicated that antibody-untreated and isotype control antibody-injected mice presented the high concentration of CD11b+Gr1^{hi} cells or CD11b+Ly6G^{hi} cells, respectively. By contrast, anti-Ly6G (Gr1) antibody-injected mice contained largely CD11b+Gr1^{int} cells with much reduced presence of CD11b+Gr1^{hi} cells. ***, $p < 0.001$; $n = 3$ in each group. *C*, the myeloid cell gate of peripheral blood samples similarly suggested that the reduction of circulating CD11b+Gr1^{hi} neutrophils in anti-Ly6G (Gr1) antibody-injected mice. ***, $p < 0.01$; $n = 3$ in each group.

Ly6G+ cells of ZOL mice were different from those of control (NaCl) mice (Fig. 3, *A* and *B*). Migration through vascular endothelial cells and the microenvironment in the local tissue can induce rapid plasticity changes in myeloid cell phenotype and function (37). It is highly conceivable that the plasticity of Ly6G+/Gr1+ cells can be significantly affected in ZOL mice. Favot *et al.* (49) examined the reactive-oxygen species (ROS) synthesis by neutrophils harvested from oral rinse and peripheral blood of ONJ patients. *N*-Formyl-methionyl-leucyl-phenylalanine (fMLP)- or phorbol myristate acetate (PMA)-stimulated ROS yield was not much different between neutrophils harvested from peripheral blood of mild (Stages 0–1) and advanced (Stages 2–3) bisphosphonate-related ONJ patients. However, oral neutrophils from ONJ patients, in particular with advanced stages, showed a reduction of ROS synthesis. Taken together, it may be suggested that the function of Ly6G+/Gr1+ cells may be modulated locally in the oral barrier tissue, particularly during the second week of tooth extraction wound healing.

The development of ONJ-like lesion occurred in the second week of tooth extraction in our ZOL-treated mouse model, characterized by the increased area of osteonecrosis interfacing the inflamed oral barrier tissue and abnormal oral epithelial hyperplasia (31, 50) (Fig. 1). The multiplex assay of cultured oral barrier cells suggested the significant reduction in secretion of cytokines and chemokines in the ZOL group at week 2 (Fig. 2*C*), which was consistent with the previously reported microarray-based transcriptome assay of the mouse oral barrier tissue (50). The oral barrier microenvironment of ZOL mice may be less effective for wound healing and inflammatory resolution. The abnormal cytokine and chemokine repertoire of the gingival oral barrier tissue may be involved in the ONJ development. The multiplex assay demonstrated that the control oral barrier cells secreted cytokines and chemokines, suggestive of

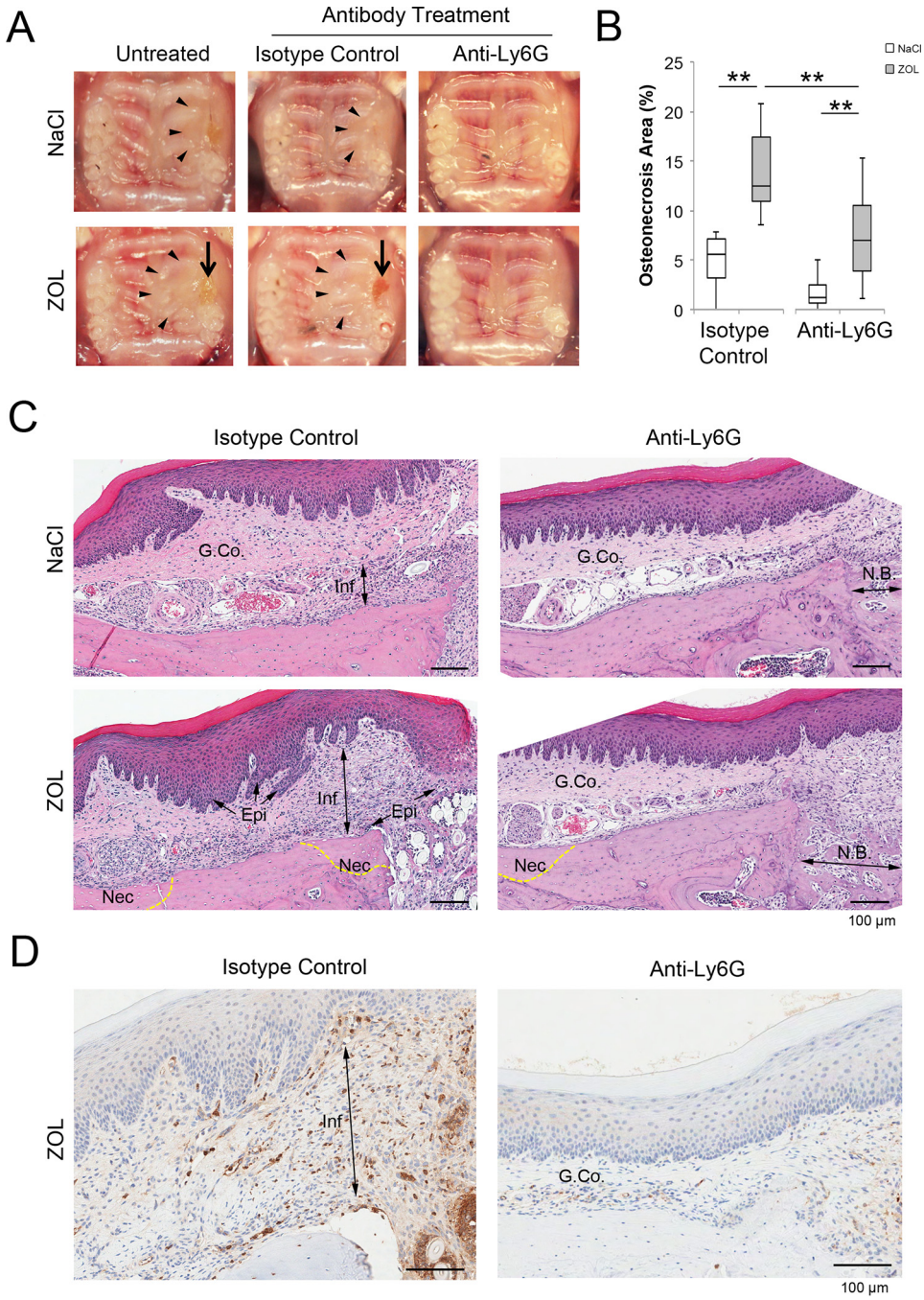

FIGURE 7. **Prevention of ONJ-like lesion by anti-Ly6G (Gr1) neutralizing antibody.** *A*, gingival swelling at the tooth extraction site (*arrowheads*) was exacerbated in ZOL mice, which also exhibited delayed wound closure (*arrows*). Mice that received isotype control antibody injection showed essentially identical reactions as the antibody-untreated mice. By contrast, anti-Ly6G (Gr1) antibody injections resulted in significantly attenuated gingival swelling in both control (NaCl) and ZOL mice. There was no open wound in anti-Ly6G (Gr1) antibody-injected ZOL mice on week 2 of tooth extraction. *B*, the area of histological osteonecrosis in the palatal bone was increased in ZOL mice. However, anti-Ly6G (Gr1) antibody injection appeared to attenuate the development of osteonecrosis. **, $p < 0.01$; $n = 6$ in each group. *C*, histological analysis revealed a localized inflammatory reaction (*Inf*, *double arrow*) in gingival connective tissue (*G.Co.*) interfacing palatal bone of control (*NaCl*) mice with the isotype control antibody injection. ZOL mice with the isotype control antibody injection exhibited not only the localized inflammation but also a large area of diffused inflammatory lesion, which was associated with osteonecrosis (*Nec*) and epithelial hyperplasia (*Epi*). Anti-Ly6G (Gr1) antibody injection resulted in the complete remission of inflammatory reaction in the gingival connective tissue interfacing palatal bone of both control (NaCl) and ZOL mice. New bone formation (*N.B.*) in the tooth extraction socket was noted in the anti-Ly6G (Gr1) antibody injection groups. *D*, immunohistochemical evaluation showed the presence of Ly6G+ cells in the diffused inflammatory zone (*Inf*, *double arrow*) of ZOL mice with isotype control antibody injection. In ZOL mice with anti-Ly6G (Gr1) antibody injection, Ly6G+ cells were not observed in the gingival connective tissue (*G.Co*) interfacing the palatal bone.

increased immunity (53), which can improve barrier immunity (54) and stimulate alternative macrophage activation (55) and epithelial cell turnover (56).

We further investigated if the abnormal oral barrier immune factors in ZOL mice may play a role in developing osteonecrosis. The condition medium of oral barrier cells dissociated from

ZOL mice induced increased necrotic reaction in murine osteocyte-like MLO-Y4 cells *in vitro* (Fig. 4*B*).

The presence of bisphosphonates in osteocyte lacunae has been shown, whereas osteocytes were not necrotic, suggesting that bisphosphonates may not have the direct effect for osteonecrosis (57). We previously reported that bisphosphonate-affected osteoclasts secreted proinflammatory cytokines (50), which appeared to locate adjacent to the osteonecrosis area (31) (Fig. 1). This study highlighted the presence of Ly6G+/Gr1+ myeloid cells in the oral barrier tissue during the tooth extraction wound healing, which may undergo local plasticity. Taken together, the pathological development of ONJ may be induced by compounded environments involving distribution of bisphosphonate and osteoclast immunity. We further propose that aberrant myeloid cell plasticity in the oral barrier tissue and abnormal oral immunity may lead to a localized trigger initiating osteonecrosis in jawbone. In conclusion, this study suggests that local modulation and possible normalization of myeloid cell plasticity in the oral barrier tissue may provide the basis for therapeutic and preventive strategy toward ONJ.

Experimental Procedures

Ethics Statement—The UCLA Animal Research Committee reviewed and approved all experimental protocols involving animals (ARC 1997–136).

ZOL Injection and Molar Tooth Extraction in Mice—A mouse model developing ONJ-like lesion was previously reported (31). Briefly, 7-week-old female C57Bl/6J mice (The Jackson Laboratory, Bar Harbor, ME) received a bolus injection of 500 μg/kg ZOL (Reclast, Novartis, East Hanover, NJ), whereas control mice received a 0.9% NaCl vehicle injection through the retro-orbital venous plexus (Fig. 1*A*). Ten days later, the maxillary left first molar was extracted under isoflurane anesthesia using a dental explorer. Analgesic agent, carprofen (5.0 mg/kg) was subcutaneously injected immediately before tooth extraction and every 24 h for 48 h after tooth extraction. Mice were euthanized at the predetermined time of tooth extraction as described below. One femur bone from each mouse was harvested, fixed in 10% buffered formalin, and evaluated by micro-CT (μCT40, Scanco Medical, Basserdorf, Switzerland) at an x-ray energy level of 55 peak kV with an intensity of 145 μA. The trabecular bone morphometry was evaluated by the proprietary algorithm (Scanco Medical). We characterized the femur structure in all animals in this experiment to ensure the reproducible and consistent effect of ZOL in compliance with the National Institutes of Health guidelines on Authentication of Key Biological and/or Chemical Resources.

Osteonecrosis Measurement at Tooth Extraction Site—Mice were euthanized by 100% CO_2 inhalation on day 3, week 2, and week 4 after tooth extraction. The maxilla containing the tooth extraction wound was harvested. After standardized digital photo recording, the maxillary tissues were fixed in 10% buffered formalin and subjected to micro-CT imaging. The fixed maxillary tissues were further decalcified with 10% EDTA (pH 7.0) for 7–10 days before the paraffin-embedded histological sample preparation. Serial cross-sections (4 μm thick) through the frontal plane including the tooth extraction site and the contralateral first molar were stained with hematoxylin and eosin (H&E) and scanned by a high throughput imaging system (Ariol SL-50, Applied Imaging, Grand Rapids, MI). The osteonecrosis area was defined by a cluster of four or more non-vital osteocytes (*i.e.* empty osteocyte lacunae or pyknotic osteocytes). The osteonecrosis area within the palatal bone was standardized by the bone area.

Osteoclast Measurement at Tooth Extraction Site—After deparaffinization, histological sections of mouse maxilla were stained with tartrate-resistant acid phosphatase (TRAP) using a commercially available kit (Sigma) at 37 °C for 2∼4 h. Nuclei were stained with hematoxylin. After staining, all slides were rinsed in 1% HCl alcohol to release the background and 1% $NaHCO_3$ solution for recovery of hematoxylin staining for 3∼5 s in sequence. Osteoclasts (OC) were defined as TRAP-positive large cells with multiple nuclei (>2 nuclei) on the bone surface. The number of OC on the surface of the palatal bone and in the bone marrow was separately counted. The number of OC was standardized by the bone surface linear length. The surface length of palatal bone or bone marrow was measured using an image-processing program (Image J, National Institutes of Health, Bethesda, MD). An operator blinded to the condition performed the histological evaluation.

Flow Cytometric Analysis of Dissociated Oral Barrier Immune Cells—The gingival oral barrier tissue including the tooth extraction wound was harvested from freshly isolated mouse maxilla on day 3, week 2, and week 4 of tooth extraction, and the gingiva tissues were immediately cut into 1-mm^3 pieces and placed into a digestion buffer containing 1 mg/ml collagenase II, 10 units/ml DNase I, and 1% bovine serum albumin in DMEM and incubated for 20 min at 37 °C on a 150 rpm shaker. After digestion, the sample was filtered through a 40-μm cell strainer and centrifuged at 1500 rpm for 10 min at 4 °C. The pellet was resuspended in DMEM, and cells were counted. In this experiment, dissociated oral barrier cells from two mice were combined in the each group of each time point. The dissociated cells were washed and incubated with fluorescent-conjugated anti-mouse CD45 and CD3 antibodies (BioLegend, San Diego, CA). IgG2b was used as the isotype control. After 30 min of incubation, the antibody-stained cells were washed and analyzed by flow cytometry (EPICS XL-MCL, Coulter, Miami, FL). The data were evaluated on a computer software package (FlowJo vX, Flowjo, Ashland, OR). This experiment was performed in three different settings.

Multiplex Cytokine/Chemokine Assay—The dissociated cells from gingival oral barrier tissue harvested on day 3, week 2, and week 4 of tooth extraction were cultured in the presence of IL-2 (10,000 units/ml) using RPMI 1640 media (Life Technologies) supplemented with 5% fetal bovine serum, 10% antibiotics/antimycotics, 1% sodium pyruvate, and 1% non-essential amino acids. The culture media were collected after 3 days, and the level of cytokines and chemokines was examined by a commercially available multiplex assay (MILLIPLEX® MAP Mouse Cytokine/Chemokine Magnetic Bead Panel, EMD Millipore, Billerica, MA). To determine the cytokine concentrations a standard curve was generated by 3-fold dilution of recombinant cytokines provided by the manufacturer. Analysis was performed using a Luminex multiplexing instrument (MAGPIX,

Millipore, Billerica, MA), and the data were analyzed by the proprietary software (xPONENT 4.2, Millipore, Billerica, MA).

Ly6G+/Gr1+ Cells in the Oral Barrier Tissue—Histological cross-sections of maxilla were deparaffinized and treated for an antigen retrieval procedure with citrate buffer (pH 6.0) and high heat for 2 min followed by a conventional blocking process. Anti-mouse Ly6G antibody (Purified Rat Anti-Mouse Ly-6G, BD Biosciences) was diluted to 1:1500 in blocking buffer and applied to the sections. After a series of washes, the secondary antibody incubation and 3,3′-diaminobenzidine chromogenic reaction were performed. The number of Ly6G+ cells in the oral barrier tissue was counted and normalized by the cross-sectional area of the oral barrier tissue.

Separately, the dissociated oral barrier cells harvested at week 2 of tooth extraction were incubated with fluorescent-conjugated anti-mouse GR1 and CD11b antibodies (BioLegend) and analyzed by flow cytometry (EPICS XL-MCL). The data were evaluated on a computer software package (FlowJo vX) as described above.

Mouse Osteocyte (MLO-Y4) Viability with Condition Media of Oral Barrier Cells from NaCl- or ZOL-treated Mice—To test the effect of immunological factors of oral barrier cells on the pathogenesis of osteonecrosis, murine osteocyte-like cells (MLO-Y4) (58) were incubated with the condition medium of dissociated oral barrier cells from NaCl (control) or ZOL mice. MLO-Y4 cells were expanded according to the supplier's protocol (Kerafast, Boston, MA). In the initial study, MLO-Y4 cells were incubated with a known agent to induce apoptosis or necrosis, cisplatin (CDDP) or HEMA, respectively. MLO-Y4 cells in 24-well plates were incubated with the condition medium for 24 h. After photographing, cells were trypsinized and washed twice with cold cell staining buffer and resuspended in annexin V binding buffer (BioLegend). Cells were then incubated with FITS-annexin V followed by phosphatidylethanolamine-propidium iodide (PI) or 7-aminoactinomycin D (7-AAD). After incubation at room temperature in the dark for 15 min, annexin V binding buffer was added to each tube and analyzed by the flow cytometry.

Myeloid Cells in Femur Bone Marrow and Peripheral Blood—Mice were euthanized on day 3, week 2, and week 4 of tooth extraction as described above. Peripheral blood samples were obtained by heart puncture, and peripheral blood mononuclear cells were isolated by Ficoll density centrifugation. Bone marrow cells were obtained from femur by flushing with PBS containing 1% FBS. Washed cells were incubated with fluorescent-conjugated anti-mouse CD11b, Ly6G, and Ly6C antibodies (BioLegend). After antibody incubation, cells were analyzed by flow cytometry and analyzed on the computer software page as described above.

Intraperitoneal Injection of Anti-Ly6G Antibody—To further test the role of Ly6G+/Gr1+ cells on the tooth extraction wound healing, we injected anti-Ly6G (Gr1) antibody (InVivoPlus anti-mouse Ly6G (Gr-1), Bio X Cell, West Lebanon, NH). Mice were pretreated with ZOL ($n = 3$) or 0.9% NaCl ($n = 3$) followed by maxillary left first molar extraction as described above. A group of mice received daily i.p. injections of anti-Ly6G antibody (300 μg/animal) from day 9 to day 13 of tooth extraction. Another group of mice ($n = 3$ in each group) received i.p. injections of isotype control antibody (InVivoPlus Rat IgG2b Isotope control anti-KLH, Clone LTF-2, Bio X Cell). All mice were euthanized on week 2 (or day 14) of tooth extraction, and the maxillary tissue was harvested. The wound healing and the area of osteonecrosis were evaluated as described above. Separately, peripheral blood and bone marrow cells were evaluated by flow cytometry.

Statistical Analysis—The data derived from multiple samples per group were presented as the mean ± S.E. Statistical comparison was made between control (NaCl) and ZOL group using Student's *t* test. *, $p < 0.05$; **, $p < 0.01$; ***, $p < 0.001$; ****, $p < 0.0001$.

Author Contributions—I. N. and A. J., in consultation with J. L., designed this study and determined the logistics of experiments. Y. S., Ka. K., Ke. K., S. P., K. M., A. H., A. J., and I. N. performed the experiment. I. N., A. J., Y. S., Ka. K., A. K., and W. H. M. analyzed and interpreted the data. I. N., A. J., Y. S., and Ka. K. drafted the manuscript. All authors agreed on the content of the manuscript. I. N. accepts responsibility for the integrity of the data analysis.

Acknowledgments—We thank the Tissue Procurement Core Laboratory, Department of Pathology and Laboratory Medicine, David Geffen School of Medicine at UCLA for histopathological and immunohistochemical specimen preparation. We also thank Jessica Cook, UCLA, for excellent technical assistance. This work was conducted in part in a facility supported by National Institutes of Health Grant C06 RR014529 from the National Center for Research Resources Research Improvement Program Grant.

References

1. Peterson, L. W., and Artis, D. (2014) Intestinal epithelial cells: regulators of barrier function and immune homeostasis. *Nat. Rev. Immunol.* **14,** 141–153
2. Segre, J. A. (2006) Epidermal barrier formation and recovery in skin disorders. *J. Clin. Invest.* **116,** 1150–1158
3. Matsui, T., and Amagai, M. (2015) Dissecting the formation, structure and barrier function of the stratum corneum. *Int. Immunol.* **27,** 269–280
4. Kagnoff, M. F. (2014) The intestinal epithelium is an integral component of a communications network. *J. Clin. Invest.* **124,** 2841–2843
5. Park, C. O., and Kupper, T. S. (2015) The emerging role of resident memory T cells in protective immunity and inflammatory disease. *Nat. Med.* **21,** 688–697
6. Sheridan, B. S., and Lefrançois, L. (2011) Regional and mucosal memory T cells. *Nat. Immunol.* **12,** 485–491
7. Gasteiger, G., Fan, X., Dikiy, S., Lee, S. Y., and Rudensky, A. Y. (2015) Tissue residency of innate lymphoid cells in lymphoid and nonlymphoid organs. *Science* **350,** 981–985
8. Hashimoto, D., Chow, A., Noizat, C., Teo, P., Beasley, M. B., Leboeuf, M., Becker, C. D., See, P., Price, J., Lucas, D., Greter, M., Mortha, A., Boyer, S. W., Forsberg, E. C., Tanaka, M., *et al.* (2013) Tissue-resident macrophages self-maintain locally throughout adult life with minimal contribution from circulating monocytes. *Immunity* **38,** 792–804
9. Fournier, B. M., and Parkos, C. A. (2012) The role of neutrophils during intestinal inflammation. *Mucosal. Immunol.* **5,** 354–366
10. Kim, N. D., and Luster, A. D. (2015) The role of tissue resident cells in neutrophil recruitment. *Trends Immunol.* **36,** 547–555
11. Soumelis, V., Pattarini, L., Michea, P., and Cappuccio, A. (2015) Systems approaches to unravel innate immune cell diversity, environmental plasticity and functional specialization. *Curr. Opin. Immunol.* **32,** 42–47
12. Kruger, P., Saffarzadeh, M., Weber, A. N., Rieber, N., Radsak, M., von Bernuth, H., Benarafa, C., Roos, D., Skokowa, J., and Hartl, D. (2015) Neutrophils: between host defense, immune modulation, and tissue injury.

PLoS Pathog. **11,** e1004651
13. Ashhurst, T. M., van Vreden, C., Niewold, P., and King, N. J. (2014) The plasticity of inflammatory monocyte responses to the inflamed central nervous system. *Cell Immunol.* **291,** 49–57
14. Scapini, P., and Cassatella, M. A. (2014) Social networking of human neutrophils within the immune system. *Blood* **124,** 710–719
15. Didierlaurent, A., Simonet, M., and Sirard, J. C. (2005) Innate and acquired plasticity of the intestinal immune system. *Cell. Mol. Life Sci.* **62,** 1285–1287
16. Omenetti, S., and Pizarro, T. T. (2015) The Treg/Th17 axis: a dynamic balance regulated by the gut microbiome. *Front. Immunol.* **6,** 639
17. Hirahara, K., Poholek, A., Vahedi, G., Laurence, A., Kanno, Y., Milner, J. D., and O'Shea, J. J. (2013) Mechanisms underlying helper T-cell plasticity: implications for immune-mediated disease. *J. Allergy Clin. Immunol.* **131,** 1276–1287
18. Gatzka, M., and Scharffetter-Kochanek, K. (2015) T-cell plasticity in inflammatory skin diseases: the good, the bad, and the chameleons. *J. Dtsch. Dermatol. Ges.* **13,** 647–652
19. Cortés-Vieyra, R., Rosales, C., and Uribe-Querol, E. (2016) Neutrophil functions in periodontal homeostasis. *J. Immunol. Res.* **2016,** 1396106
20. Lin, A., Hokugo, A., Choi, J., and Nishimura, I. (2010) Small cytoskeleton-associated molecule, fibroblast growth factor receptor 1 oncogene partner 2/wound inducible transcript-3.0 (FGFR1OP2/wit3.0), facilitates fibroblast-driven wound closure. *Am. J. Pathol.* **176,** 108–121
21. Lin, A., Hokugo, A., and Nishimura, I. (2010) Wound closure and wound management: A new therapeutic molecular target. *Cell Adh. Migr.* **4,** 396–399
22. Nathan, C. (2006) Neutrophils and immunity: challenges and opportunities. *Nat. Rev. Immunol.* **6,** 173–182
23. Scott, D. A., and Krauss, J. (2012) Neutrophils in periodontal inflammation. *Front. Oral Biol.* **15,** 56–83
24. Ruggiero, S. L., Dodson, T. B., Fantasia, J., Goodday, R., Aghaloo, T., Mehrotra, B., O'Ryan, F., and American Association of Oral and Maxillofacial Surgeons (2014) American Association of Oral and Maxillofacial Surgeons position paper on medication-related osteonecrosis of the jaw–2014 update. *J. Oral Maxillofac. Surg.* **72,** 1938–1956
25. Khosla, S., Burr, D., Cauley, J., Dempster, D. W., Ebeling, P. R., Felsenberg, D., Gagel, R. F., Gilsanz, V., Guise, T., Koka, S., McCauley, L. K., McGowan, J., McKee, M. D., Mohla, S., *et al.* (2007) Bisphosphonate-associated osteonecrosis of the jaw: report of a task force of the American Society for Bone and Mineral Research. *J. Bone Miner Res.* **22,** 1479–1491
26. Baron, R., Ferrari, S., and Russell, R. G. (2011) Denosumab and bisphosphonates: different mechanisms of action and effects. *Bone* **48,** 677–692
27. Russell, R. G., Xia, Z., Dunford, J. E., Oppermann, U., Kwaasi, A., Hulley, P. A., Kavanagh, K. L., Triffitt, J. T., Lundy, M. W., Phipps, R. J., Barnett, B. L., Coxon, F. P., Rogers, M. J., Watts, N. B., and Ebetino, F. H. (2007) Bisphosphonates: an update on mechanisms of action and how these relate to clinical efficacy. *Ann. N.Y. Acad. Sci.* **1117,** 209–257
28. Utreja, A., Almas, K., and Javed, F. (2013) Dental extraction as a risk factor for bisphosphonate related osteonecrosis of the jaw in cancer patients: an update. *Odontostomatol. Trop.* **36,** 38–46
29. Yamazaki, T., Yamori, M., Ishizaki, T., Asai, K., Goto, K., Takahashi, K., Nakayama, T., and Bessho, K. (2012) Increased incidence of osteonecrosis of the jaw after tooth extraction in patients treated with bisphosphonates: a cohort study. *Int. J. Oral Maxillofac. Surg.* **41,** 1397–1403
30. Hokugo, A., Christensen, R., Chung, E. M., Sung, E. C., Felsenfeld, A. L., Sayre, J. W., Garrett, N., Adams, J. S., and Nishimura, I. (2010) Increased prevalence of bisphosphonate-related osteonecrosis of the jaw with vitamin D deficiency in rats. *J. Bone Miner Res.* **25,** 1337–1349
31. Park, S., Kanayama, K., Kaur, K., Tseng, H. C., Banankhah, S., Quje, D. T., Sayre, J. W., Jewett, A., and Nishimura, I. (2015) Osteonecrosis of the jaw developed in mice: disease variants regulated by γδ T cells in oral mucosal barrier immunity. *J. Biol. Chem.* **290,** 17349–17366
32. Ali, N., Jurczyluk, J., Shay, G., Tnimov, Z., Alexandrov, K., Munoz, M. A., Skinner, O. P., Pavlos, N. J., and Rogers, M. J. (2015) A highly sensitive prenylation assay reveals *in vivo* effects of bisphosphonate drug on the Rab prenylome of macrophages outside the skeleton. *Small GTPases* **6,** 202–211
33. Hoefert, S., Hoefert, C. S., Albert, M., Munz, A., Grimm, M., Northoff, H., Reinert, S., and Alexander, D. (2015) Zoledronate but not denosumab suppresses macrophagic differentiation of THP-1 cells. An aetiologic model of bisphosphonate-related osteonecrosis of the jaw (BRONJ). *Clin. Oral Investig.* **19,** 1307–1318
34. Failli, A., Legitimo, A., Orsini, G., Romanini, A., and Consolini, R. (2014) The effects of zoledronate on monocyte-derived dendritic cells from melanoma patients differ depending on the clinical stage of the disease. *Hum. Vaccin. Immunother.* **10,** 3375–3382
35. Kalyan, S., Chandrasekaran, V., Quabius, E. S., Lindhorst, T. K., and Kabelitz, D. (2014) Neutrophil uptake of nitrogen-bisphosphonates leads to the suppression of human peripheral blood γδ T cells. *Cell Mol. Life Sci.* **71,** 2335–2346
36. Kuiper, J. W., Forster, C., Sun, C., Peel, S., and Glogauer, M. (2012) Zoledronate and pamidronate depress neutrophil functions and survival in mice. *Br. J. Pharmacol.* **165,** 532–539
37. Galli, S. J., Borregaard, N., and Wynn, T. A. (2011) Phenotypic and functional plasticity of cells of innate immunity: macrophages, mast cells and neutrophils. *Nat. Immunol.* **12,** 1035–1044
38. Scapini, P., Lapinet-Vera, J. A., Gasperini, S., Calzetti, F., Bazzoni, F., and Cassatella, M. A. (2000) The neutrophil as a cellular source of chemokines. *Immunol. Rev.* **177,** 195–203
39. Arora, M., Poe, S. L., Oriss, T. B., Krishnamoorthy, N., Yarlagadda, M., Wenzel, S. E., Billiar, T. R., Ray, A., and Ray, P. (2010) TLR4/MyD88-induced CD11b+Gr-1 int F4/80+ non-migratory myeloid cells suppress Th2 effector function in the lung. *Mucosal. Immunol.* **3,** 578–593
40. Obregón-Henao, A., Henao-Tamayo, M., Orme, I. M., and Ordway, D. J. (2013) Gr1(int)CD11b+ myeloid-derived suppressor cells in Mycobacterium tuberculosis infection. *PLoS ONE* **8,** e80669
41. Talmadge, J. E., and Gabrilovich, D. I. (2013) History of myeloid-derived suppressor cells. *Nat. Rev. Cancer* **13,** 739–752
42. Sagiv, J. Y., Michaeli, J., Assi, S., Mishalian, I., Kisos, H., Levy, L., Damti, P., Lumbroso, D., Polyansky, L., Sionov, R. V., Ariel, A., Hovav, A. H., Henke, E., Fridlender, Z. G., and Granot, Z. (2015) Phenotypic diversity and plasticity in circulating neutrophil subpopulations in cancer. *Cell Rep.* **10,** 562–573
43. Rose, S., Misharin, A., and Perlman, H. (2012) A novel Ly6C/Ly6G-based strategy to analyze the mouse splenic myeloid compartment. *Cytometry A* **81,** 343–350
44. Ueda, Y., Kondo, M., and Kelsoe, G. (2005) Inflammation and the reciprocal production of granulocytes and lymphocytes in bone marrow. *J. Exp. Med.* **201,** 1771–1780
45. Scumpia, P. O., Kelly-Scumpia, K. M., Delano, M. J., Weinstein, J. S., Cuenca, A. G., Al-Quran, S., Bovio, I., Akira, S., Kumagai, Y., and Moldawer, L. L. (2010) Cutting edge: bacterial infection induces hematopoietic stem and progenitor cell expansion in the absence of TLR signaling. *J. Immunol.* **184,** 2247–2251
46. Szpaderska, A. M., Zuckerman, J. D., and DiPietro, L. A. (2003) Differential injury responses in oral mucosal and cutaneous wounds. *J. Dent. Res.* **82,** 621–626
47. Menzies-Gow, A., Ying, S., Sabroe, I., Stubbs, V. L., Soler, D., Williams, T. J., and Kay, A. B. (2002) Eotaxin (CCL11) and eotaxin-2 (CCL24) induce recruitment of eosinophils, basophils, neutrophils, and macrophages as well as features of early- and late-phase allergic reactions following cutaneous injection in human atopic and nonatopic volunteers. *J. Immunol.* **169,** 2712–2718
48. Rovai, L. E., Herschman, H. R., and Smith, J. B. (1998) The murine neutrophil-chemoattractant chemokines LIX, KC, and MIP-2 have distinct induction kinetics, tissue distributions, and tissue-specific sensitivities to glucocorticoid regulation in endotoxemia. *J. Leukoc. Biol.* **64,** 494–502
49. Favot, C. L., Forster, C., and Glogauer, M. (2013) The effect of bisphosphonate therapy on neutrophil function: a potential biomarker. *Int. J. Oral Maxillofac. Surg.* **42,** 619–626
50. Tseng, H. C., Kanayama, K., Kaur, K., Park, S. H., Park, S., Kozlowska, A., Sun, S., McKenna, C. E., Nishimura, I., and Jewett, A. (2015) Bisphosphonate-induced differential modulation of immune cell function in gingiva and bone marrow *in vivo*: role in osteoclast-mediated NK cell activation.

Oncotarget **6,** 20002–20025
51. Wicks, K., Torbica, T., Umehara, T., Amin, S., Bobola, N., and Mace, K. A. (2015) Diabetes Inhibits Gr-1+ myeloid cell maturation via cebpa deregulation. *Diabetes* **64,** 4184–4197
52. Bannon, P., Wood, S., Restivo, T., Campbell, L., Hardman, M. J., and Mace, K. A. (2013) Diabetes induces stable intrinsic changes to myeloid cells that contribute to chronic inflammation during wound healing in mice. *Dis. Model Mech.* **6,** 1434–1447
53. Wynn, T. A. (2015) Type 2 cytokines: mechanisms and therapeutic strategies. *Nat. Rev. Immunol.* **15,** 271–282
54. Chiaramonte, M. G., Schopf, L. R., Neben, T. Y., Cheever, A. W., Donaldson, D. D., and Wynn, T. A. (1999) IL-13 is a key regulatory cytokine for Th2 cell-mediated pulmonary granuloma formation and IgE responses induced by *Schistosoma mansoni* eggs. *J. Immunol.* **162,** 920–930
55. Anthony, R. M., Urban, J. F., Jr., Alem, F., Hamed, H. A., Rozo, C. T., Boucher, J. L., Van Rooijen, N., and Gause, W. C. (2006) Memory T(H)2 cells induce alternatively activated macrophages to mediate protection against nematode parasites. *Nat. Med.* **12,** 955–960
56. Cliffe, L. J., Humphreys, N. E., Lane, T. E., Potten, C. S., Booth, C., and Grencis, R. K. (2005) Accelerated intestinal epithelial cell turnover: a new mechanism of parasite expulsion. *Science* **308,** 1463–1465
57. Roelofs, A. J., Coxon, F. P., Ebetino, F. H., Lundy, M. W., Henneman, Z. J., Nancollas, G. H., Sun, S., Blazewska, K. M., Bala, J. L., Kashemirov, B. A., Khalid, A. B., McKenna, C. E., and Rogers, M. J. (2010) Fluorescent risedronate analogues reveal bisphosphonate uptake by bone marrow monocytes and localization around osteocytes *in vivo*. *J. Bone Miner Res.* **25,** 606–616
58. Kato, Y., Windle, J. J., Koop, B. A., Mundy, G. R., and Bonewald, L. F. (1997) Establishment of an osteocyte-like cell line, MLO-Y4. *J. Bone Miner Res.* **12,** 2014–2023